Two-Dimensional Colloid Crystals Obtained by Coupling of Flow and Confinement

Eugenia Kumacheva,[1,2] Piotr Garstecki,[1] Hongkai Wu,[1] and George M. Whitesides[1,*]

[1]*Chemistry & Chemical Biology Department, Harvard University, 12 Oxford Street, Cambridge, Massachusetts 02138, USA*
[2]*Department of Chemistry, University of Toronto, 80 Saint George Street, Toronto, Ontario, Canada M5S3H6, USA*

(Received 27 January 2003; published 19 September 2003)

This Letter describes the generation of 2D colloidal lattices in microchannels by coupling the laminar flow of dispersions of spherical colloids and geometrical confinement. We describe a nonequilibrium, convective, mechanism leading to formation of ordered 2D structures of both closed-packed hexagonal and non-closed-packed rhombic symmetries. The number and types of possible lattices is determined by the ratio of the width of the channel to the diameter of the particle. The structures tend to return to a regular lattice after a defect is introduced; that is, for example, they tend to self-repair disorder induced by particle polydispersity, contaminants, and flow instabilities. The stability of different lattices is analyzed numerically for particles with different polydispersity.

DOI: 10.1103/PhysRevLett.91.128301 PACS numbers: 82.70.Dd, 61.44.–n, 68.90.+g, 81.16.–c

Confinement-induced crystallization is a subject of current interest, since it provides a route to periodic structures, and allows the study of many-body interactions [1–3]. Planar, micron-scale patterns can template the crystallization of colloid particles both "in-plane" and "out-of-plane," in processes driven by gravitational, capillary, or electrohydrodynamic forces [3]. These processes generate close-packed structures: hexagonal 2D lattices, and hcp or fcc 3D lattices. We describe the convective growth of 2D colloidal lattices. We report formation of non-closed-packed structures, which have not been observed previously in self-assembly of microspheres. By contrast with other nonequilibrium growth processes (e.g., percolation [4], diffusion-limited aggregation [5], or cluster-cluster aggregation [6]), we obtain ordered, periodic lattices with the geometry of the unit cell controlled by the dimensions of the microfluidic channel.

Formation of lattices in our experiments is an intrinsically nonequilibrium process. Assuming that the system is close to equilibrium and stationary, the resulting lattices should satisfy the postulate of the minimum entropy production rate [7]. The energy of the particles in the hydrodynamic drag field is, however, larger than kT by several orders of magnitude. The combination of geometrical confinement with unidirectional flow causes kinetic entrapment of the ordered structures. The resulting 2D lattices are therefore not an equilibrium solution yielding a minimum of the appropriate energy functional (for example, maximization of the interparticle contact area, or the compactness of the structure). They satisfy only the local minimal energy dissipation rate postulate. As we use dilute suspensions of the microspheres, the particles enter the channel one at a time, and the configurational degrees of freedom are effectively reduced to the order in which the beads are deposited.

Figure 1(a) illustrates schematically the organization of microspheres in the microfluidic geometry. The microchannel ends with one or more outlets narrower than the diameter of the microbead. When a suspension is forced through the channel, the particles deposit irreversibly at the end, and nucleate the growth of a 2D lattice.

The flow of fluid through the voids between particles can be considered as laminar flow through parallel capillaries [8] (in our experiments the Reynolds number, Re, had values between 10 and 100). New particles approaching the array flow passively and move to the interstitial voids between the beads that have already assembled. The voids in each layer act as a template to position the beads in the next one. Meakin and Jullien predicted [9] that, for monodisperse beads, this mechanism would lead to a variety of lattices with large repeating units and packings unstable with respect to small perturbations in particle

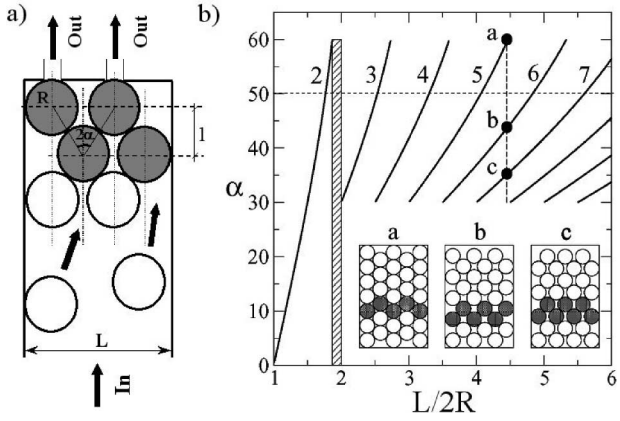

FIG. 1. (a) Flow-driven organization of spherical particles in a microchannel. The shaded beads constitute the repeating unit. The interlayer spacing l is shown on the right. (b) Diagram of possible regular phases obtained for particles with radius R for different values of $L/2R$. Each solid line corresponds to a given number of particles n in a repeating unit. In the dashed area no regular structures can be formed. Inset: Possible lattices obtained for $L/2R = 4.46$.

 0031-9007/03/91(12)/128301(4)$20.00

coordinates. In our experiments, we observed small numbers of stable, regular structures with small repeating units. The difference between the experimental results and the simulations arises from the fact that, in the simulations, the beads are ideally monodisperse and are deposited at, within the numerical accuracy, "ideal" positions. In the experiment, beads have a finite polydispersity. This polydispersity can be viewed as a measure of the perturbations introduced into an otherwise perfect lattice. To our surprise, we observe that finite polydispersity in fact stabilizes the lattices composed of small repeat units.

The relationship between the width of the channel L, the radius of a microbead R, the angle α, and the number of "columns" n, parallel to the direction of flow [vertical dashed lines in Fig. 1(a)] is $L = 2R[(n-1)\sin\alpha + 1]$. The number of possible regular structures is determined by the ratio of the width of the channel L to the particle diameter $2R$ [Fig. 1(b)]. A structure with a particular value of α can be preserved only for discrete values of the ratios $L/2R$ [indicated by the horizontal dashed line in Fig. 1(b)]. The solid lines show the dependence of α on $L/2R$ for a particular number of beads in the repeating unit ($n = \text{const}$); as the width of the channel increases, the lattice transforms from hexagonal ($\alpha = 30°$) to rhombic, and then again to hexagonal ($\alpha = 60°$).

The most interesting situation occurs for $L = \text{const}$. For $L/2R > 2.5$, more than one ordered structure can form in a single channel. For example, we anticipate three lattices for $L/2R = 4.46$ [indicated by the vertical dashed line in Fig. 1(b), and by the inset]. On the basis of the diagram, hexagonal lattices form only when $L/2R = (n+1)/2$ (for $\alpha = 30°$) and when $L/2R = 1 + (n-1)(\sqrt{3/2})$ (for $\alpha = 60°$).

We used soft lithography [10] to create microchannels in poly(dimethylsiloxane) sheet, which we sealed to a glass substrate. Experiments were conducted with aqueous dispersions of polystyrene beads (Duke Scientific). Average diameters of the particles were 40, 80, and 100 μm, with standard deviations of 0.6, 0.8, and 1.6 μm, respectively. A colloidal dispersion with particle concentration 0.2 wt % was pumped through the channels using flow rates from 0.05 to 3.0 mL/ min. The density of water was matched to the density of polystyrene ($\rho = 1.05\ \text{g/cm}^3$) by introducing KBr into the aqueous medium. The structure of particle arrays was imaged with a Leica DMRX microscope, coupled with a Nikon CCD camera NXM1200.

Figure 2 shows representative fragments of the 2D lattices obtained from 100-μm spheres in microchannels with height 130 μm and widths between 207 and 463 μm. In channels with $L/2R = 2.22$ and $L/2R = 3.33$ [Figs. 2(a) and 2(c)], we observed only rhombic lattices, with $\alpha = 37°$ and 50°, respectively. These values of α were expected from the diagram [Fig. 1(b)]; for $L/2R = 3.33$, however, the second rhombic structure

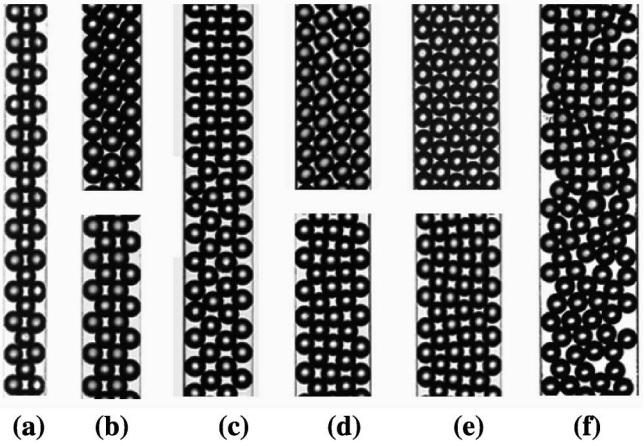

FIG. 2. Fragments of 2D lattices generated from 100-μm beads in microchannels with $L/2R$: (a) 2.20, (b) 2.65, (c) 3.33, (d) 3.71, (e) 4.46; (f) 5.11. Flow rate was 0.5 mL/ min.

with $\alpha = 34°$ did not form. For $L/2R$ equal to 2.65, 3.71, or 4.46, both rhombic and close-to-hexagonal lattices were observed [Figs. 2(b), 2(d), and 2(e)]. We have found that, out of the possible structures predicted by geometrical considerations, those with a larger value of α were formed more often. For example, for $L/2R = 4.46$, we have not observed the lattice with seven beads in the repeating unit ($\alpha = 35.2°$). For $L/2R = 5.11$, the organization of particles became disordered. For this $L/2R$ ratio, the diagram in Fig. 1(b) predicted four lattices. In general, we observe that as the ratio $L/2R$ and the number of possible lattices increase the system switches between the different structures more often. As a result, for $L/2R > 5$ the organization of beads is largely disordered.

The lattices formed from 40- and 80-μm beads were similar to the lattices in Fig. 2. Figure 3 shows the variation in α for rhombic structures obtained from 40-, 80-, and 100-μm beads in channels with $2 < L/2R < 3$.

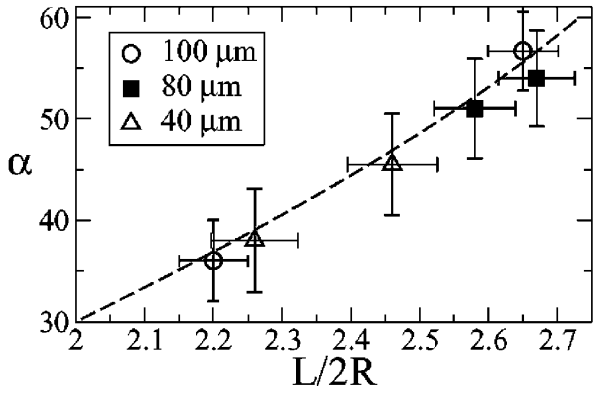

FIG. 3. Variation in angle α versus normalized channel width $L/2R$ for lattices containing three particles in the repeating unit. The dashed line shows the variation in α estimated from Fig. 1(b).

For $n = 3$, experimental values of α correlated with the expected ones. We did not, however, observe lattices with $\alpha \leq 35°$.

We summarize the characteristic features of particle assembly induced by flow in microchannels qualitatively as follows. The number of outlets at the end of the channel (from 1 to 4) did not notably affect the organization of the particles. Lattices with high periodicity formed when channel height did not exceed particle diameter by more than 30% [11]. The flow rate of the fluid was one of the major factors influencing the growth of 2D crystals. For 100-μm particles, ordered arrays formed only when the flow rate, Q, fell between ca. 0.3 to 2 mL/min, for L from 220 to 446 μm. Under these conditions, the individual beads immobilized exactly between the microspheres of the preceding layer. For $Q < 0.1$ and for $Q > 2$ mL/min, particle assembly became random.

One of the interesting features of particle assembly was "self-healing" of the periodic structures. When the outlets were intentionally positioned in a way that interfered with the growth of the colloid crystal, the organization of the beads was affected only in the first 4–6 layers along the axis of the channel; then the array reorganized and grew in a periodic fashion [Fig. 4(a)]. When defects were generated in the 2D lattice [by introducing a contaminant [Fig. 4(b)], or a large bead [Fig. 4(c)], or as the result of an instability in liquid flow [Fig. 4(d)]], the system lost its periodicity for several layers of particles, but then returned to a periodic lattice.

In microchannels accommodating both hexagonal and rhombic structures, the transitions between them occurred as a result of instabilities in flow or of the variations in the size of the microbeads. In order to examine how the polydispersity of the particles [defined as $\sigma = (\langle R^2\rangle - \langle R\rangle^2)^{1/2}/\langle R\rangle$] influences the formation of ordered lattices, we performed numerical simulations [12]. We assumed that the interaction between the particles was represented solely by hard-sphere repulsion, and did not attempt to simulate the dynamics of the flow. Our interest centered solely on geometrical packing. The starting condition was given by the first layer of randomly positioned particles. Then 1000 microbeads, with diameters drawn from a Gaussian probability distribution centered on $2\langle R\rangle$, were placed in the farthest possible positions along the direction of the flow; that is, in the voids between the beads that were already deposited.

We tested several channel widths with characteristic ratios $L/2R$. For each $L/2R \in (2, 5)$ and $\sigma \in (0, 0.15)$, 100 numerical experiments were performed. The first 100 beads were neglected. Then for each particle we examined the extent of local order around it by tracing the average vertical spacing, l [Fig. 1(a)], between the neighboring particles as $\lambda_p = (1/N)\sum_{i,j}|z_i - z_j|$, where p is the particle index, and N denotes the number of particle pairs ($N = 50$) examined. For a particular ratio $L/2R$, the diagram in Fig. 1(b) gives the number N_{latt} of possible regular lattices. Each of them was characterized by an angle $\alpha_k$where $k \in (1, N_{\text{latt}})$ and interlayer distance $l_k = 2R\cos(\alpha_k)$. In further analysis, the local structure around the pth particle was associated with the regular lattice for which $|\lambda_p - l_k|$ was the smallest. The size m of the single domain was defined as the number of beads in a particular lattice.

Figure 5 shows the results for $L/2R = 2.7$. For this ratio, we anticipated two regular structures: a close-to-hexagonal structure ($\alpha_1 = 58.2°$, $l_1/2R = 0.52$) and a rhombic lattice ($\alpha_2 = 34.5°$, $l_2/2R = 0.82$), both illustrated in Fig. 5. Figure 5(a) shows the variation in the average number of beads, $\langle m\rangle$, in a single ordered domain versus σ. The value of $\langle m\rangle$ rapidly decreased with

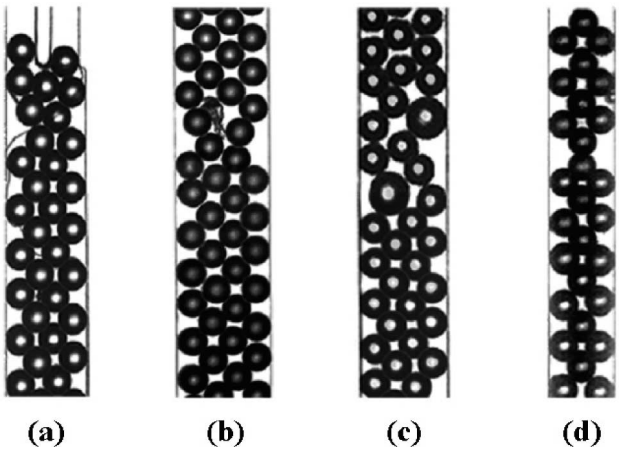

FIG. 4. Effect of local perturbations on growth of 2D lattices: (a) incommensurability of outlet position with lattice structure; (b) presence of contaminant; (c) introduction of large spheres; (d) flow instability.

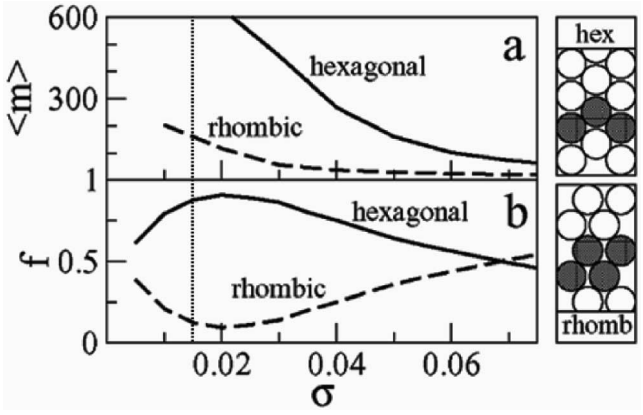

FIG. 5. Results of numerical experiments for channel width $L/2\langle R\rangle = 2.7$ for close-to-hexagonal (solid line) and rhombic (dashed line) structures: The average number of particles in a regular domain (a) and the fraction of beads in a lattice (b) are plotted versus the standard deviation σ in particle diameter. The vertical dotted line corresponds to the standard deviation of the beads used in the experiments.

increasing σ. For $0.01 < \sigma < 0.075$, the hexagonal structure exhibited a larger domain size than the rhombic one. Figure 5(b) shows the fraction of beads in each of the lattices. For small polydispersity, the probability of forming a close-to-hexagonal structure was significantly higher than the probability of forming a rhombic lattice. For $\sigma > 0.02$, however, the fraction of rhombic structures gradually increased, and for $\sigma = 0.067$ it became equal to 0.5. This result agreed with experimental observations.

The results obtained for other values of $L/2R$ were similar. In general, low polydispersity σ favored close-packed lattices, while moderately polydisperse particles assembled in rhombic structures. For $\sigma = 0.015$, which corresponds to the polydispersity of the beads used in our experiments, we found that the system preferentially formed the structure with a larger value of α [Fig. 1(b)]. This result from simulations agrees with the experimental observations: For a particular value of $L/2R$, the lattices with larger α were obtained more frequently than those with smaller α, and we have not observed formation of a structure with $\alpha < 35$.

The results described in this Letter enhance our understanding of flow-driven crystallization of colloid particles in confined geometries. Earlier studies yielded only close-packed hexagonal and square lattices [3]. Here we describe conditions for formation of a range of centered rectangular lattices. The variation in the angle α compensates for incommensurability between the channel width and particle size. We have also observed self-healing ordered arrays: After perturbations induced local disorder, the system spontaneously reverted to growth in an ordered fashion. Numerical simulations correctly predicted enhanced stability of the rhombic structures in systems comprised of moderately polydisperse beads. Non-close-packed structures of colloid beads may have applications in creation of micrometer-scale fluid pumps, particulate valves [13], and in mixing confluent streams in microfluidics systems [14].

We thank DoE (Grant No. DE-FG02-00ER45852) for financial support of this work. The Foundation for Polish Science, and Canada Research Chair Fund supported the salaries of P. G. and E. K., respectively. We are grateful to Professor Howard Stone (Harvard University) for helpful discussions.

*Author to whom correspondence may be addressed.
Electronic address: gwhitesides@gmwgroup.harvard.edu

[1] J. Klein and E. Kumacheva, Science **269**, 816 (1995); J. P. Gao, W. D. Luedtke, and U. Landman, Phys. Rev. Lett. **79**, 705 (1997); V. Zaloj, M. Urbakh, and J. Klafter, Phys. Rev. Lett. **82**, 4823 (1999); M. Heuberger, M. Zach, and N. D. Spencer, Science **292**, 9052 (2001).

[2] P. Pieranski, L. Strzelecki, and B. Pansu, Phys. Rev. Lett. **50**, 900 (1983); M. Schmidt and H. Löwen, Phys. Rev. Lett. **76**, 4552 (1996); A. Marcus and S. Rice, Phys. Rev. Lett. **77**, 2577 (1996);

[3] Y. Yin, Y. Lu, B. Gates, and Y. Xia, J. Am. Chem. Soc. **123**, 8718 (2001); G. A. Ozin and S. M. Yang, Adv. Funct. Mater. **11**, 95 (2001); E. Kumacheva, R. K. Golding, M. Allard, and E. H. Sargent, Adv. Mater. **14**, 221 (2002).

[4] *Fractals and Disordered Systems*, edited by A. Bunde and S. Havlin (Springer-Verlag, Berlin, 1991).

[5] T. A. Witten and L. M. Sander, Phys. Rev. Lett. **47**, 1400 (1981).

[6] P. Meakin, Phys. Rev. Lett. **51**, 1119 (1983).

[7] I Prigogine, Bull. Acad. Roy. Belg. Cl. Sci. **31**, 600 (1945).

[8] R. F. Probstein, *Physicochemical Hydrodynamics* (Wiley, New York, 1994).

[9] P. Meakin and R. Jullien, Europhys. Lett. **15**, 851 (1991).

[10] Y. Xia and G. M. Whitesides, Annu. Rev. Mater. Sci. **28**, 153 (1998).

[11] The smallest channel height was about 20% larger than the particle diameter.

[12] See EPAPS Document No. E-PRLTAO-91-048335 for the computer program used in simulations. A direct link to this document may be found in the online article's HTML reference section. The document may also be reached via the EPAPS homepage (http://www.aip.org/pubservs/epaps.html) or from ftp.aip.org in the directory /epaps/. See the EPAPS homepage for more information.

[13] A. Terray, J. Oakey, and D. W. M. Marr, Science **296**, 1841 (2002).

[14] G. H. Seong and R. M. Crooks, J. Am. Chem. Soc. **124**, 13 360 (2002).